



# Rational Design, Synthesis, and In Vitro Neuroprotective Evaluation of Novel Glitazones for PGC-1 $\alpha$ Activation via PPAR- $\gamma$ : a New Therapeutic Strategy for Neurodegenerative Disorders

Antony Justin<sup>1</sup> · Subhankar Mandal<sup>2</sup> · P. Prabitha<sup>2</sup> · S. Dhivya<sup>2</sup> · S. Yuvaraj<sup>2</sup> · Pradeep Kabadi<sup>3</sup> ·  
Satheesh John Sekhar<sup>1</sup> · C. H. Sandhya<sup>1</sup> · Ashish D. Wadhvani<sup>1</sup> · Selvaraj Divakar<sup>1</sup> · Jeyabalan Jeyaram Bharathi<sup>1</sup> ·  
Priya Durai<sup>2</sup> · B. R. Prashantha Kumar<sup>2</sup>

Received: 27 February 2019 / Revised: 16 October 2019 / Accepted: 25 October 2019  
© Springer Science+Business Media, LLC, part of Springer Nature 2019

## Abstract

In the present study, two structurally diverse novel glitazones were designed and synthesized for activation of central PGC-1 $\alpha$  signaling through stimulation of PPAR- $\gamma$  receptor. The functional interaction between PGC-1 $\alpha$  and PPAR- $\gamma$  is a key interaction in the normal physiology of neuroprotective mechanism. Therefore, activation of PPAR- $\gamma$ -dependent PGC-1 $\alpha$  co-activator signaling could be an effective strategy to exhibit neuroprotection in several neurodegenerative disorders like Alzheimer's disease, Parkinson's disease, and cerebral ischemia. As part of rational design, analogs were designed manually based on principles of bioisosterism, followed by virtually screened using docking to predict the mode of interaction of compound towards the binding site and molecular dynamic simulation to observe the structural changes that occur during compound interaction with active site. The designed two glitazones (**G1**, **G2**) were synthesized and structurally analyzed. As part of evaluation, synthesized glitazones were subjected for preliminary neuroprotective evaluation in Lipopolysaccharide (LPS) intoxicated SH-SY5Y neuroblastoma cells. The results indicate that pre-treatment with synthesized glitazones have increased the percentage cell viability, protected the cell morphology, and decreased the release of pro-inflammatory cytokines (IL-1 $\beta$ , TNF- $\alpha$ ), lipid peroxide (LPO), and nitric oxide (NO) level in LPS intoxicated SH-SY5Y cells. Interestingly, among the two glitazones, **G2** has shown significant neuroprotection in comparison to **G1** and neuroprotective effect exerted by **G2** was similar and comparable with the standard pioglitazone. Altogether, neuroprotection exhibited by this non-thiazolidione-based glitazones during neuroinflammatory conditions may be attributed to the activation of central PGC-1 $\alpha$  signaling via PPAR- $\gamma$  receptor.

**Keywords** PGC-1 $\alpha$  · PPAR- $\gamma$  · Glitazones · Docking · Molecular dynamic simulation · Cytokines · Free radicals

---

**Electronic supplementary material** The online version of this article (<https://doi.org/10.1007/s12640-019-00132-9>) contains supplementary material, which is available to authorized users.

---

✉ B. R. Prashantha Kumar  
brprashanthkumar@jssuni.edu.in

<sup>1</sup> Department of Pharmacology, JSS College of Pharmacy, Ooty, Tamil Nadu 643 001, India

<sup>2</sup> Department of Pharmaceutical Chemistry, JSS College of Pharmacy, Mysuru, Karnataka 570015, India

<sup>3</sup> Bioanalytical Division, Biocon Pvt. Ltd, Bengaluru 560100, India

## Introduction

Neuroinflammation refers to inflammation in the nervous tissue and it is a host defensive mechanism in the brain tissue due to infection, direct cell injury, accumulation of toxic metabolites, or autoimmunity leads to metabolic alterations within the central nervous system (CNS) (DiSabato et al. 2016). Increasing evidences are supporting the imperative role of neuroinflammation in the pathogenesis of several neurodegenerative diseases such as Alzheimer's disease (AD), Multiple sclerosis (MS), Parkinson's disease (PD), amyotrophic lateral sclerosis (ALS) and cerebral ischemia (Zhao et al. 2019). Neuroinflammation is characterized by rapid activation of microglia followed by production of pro-inflammatory

cytokines, oxy-radicals, and infiltration of various peripheral immune cells into the brain tissue and these cellular events will contribute to neurodegeneration (Jin et al. 2010). Activation of toll-like receptors-4 (TLR-4) is expressed in the microglial membranes by pathogens or host-derived molecules that initiate the neuroinflammatory pathways through activation of nuclear factor-kappa B (NF- $\kappa$ B) signal transduction pathway (Rosenberger et al. 2014). The increased expression of NF- $\kappa$ B will further trigger the release of pathophysiological factors of neuroinflammation like interleukins-1 $\beta$  (IL-1 $\beta$ ), interleukins-6 (IL-6), tumor necrosis factor- $\alpha$  (TNF- $\alpha$ ), adhesion molecules, prostaglandins, and reactive oxygen species (ROS) resulted in neurodegeneration and neuronal death (Lattke et al. 2017).

Peroxisome proliferator-activated receptors (PPARs) are members of the nuclear receptor superfamily, and they regulate various gene expressions either through ligand-dependent or independent molecular processes (Clarke et al. 1999). There are three isoforms of PPAR receptor: alpha ( $\alpha$ ), beta ( $\beta$ )/delta ( $\delta$ ), and gamma ( $\gamma$ ), all of which form obligate heterodimers with the retinoid-X-receptor (RXR), which bind to the deoxyribonucleic acid (DNA) response elements resulting in respective gene regulation (Tyagi et al. 2011). Among the three isoforms, PPAR- $\gamma$  is mainly focused by several researchers for neuroprotection due to its wide distribution in the different brain regions (Moreno et al. 2004) and exhibits anti-neuroinflammatory activity upon activation through modulating NF- $\kappa$ B signaling pathway (Choi et al. 2017). The report has shown that deficiency of neuronal PPAR- $\gamma$  receptors increases intensity of brain damage in response to cerebral ischemia (Zhao et al. 2009) and activation of PPAR- $\gamma$  by its agonist exerted neuroprotection by attenuation of brain cytokine levels in cerebral ischemic rats (Luo et al. 2006) and Parkinson's disease (Randy and Guoying 2007).

Recent evidences indicate that agonist activity at PPAR- $\gamma$  receptor has decreased the expression of autophagy-related proteins, including microtubule-associated protein 1 light chain 3 type II (LC3-II), beclin-1, and cathepsin D (Li et al. 2017) and maintains the acute mitochondrial integrity (Patel et al. 2017) in traumatic spinal cord injury animal model. Activation of PPAR- $\gamma$ -dependent signaling in advanced glycation end product treated human neural stem cells has shown neuroprotection suggesting that PPAR- $\gamma$  ligands are promising agents in the therapeutic management of patients with neurodegenerative diseases (Chiang et al. 2017). In general, stimulation of PPAR- $\gamma$  with ligands resulted in heterodimerize with RXR and recruits the proliferator-activated receptor gamma co-activator 1-alpha (PGC-1 $\alpha$ ) to form a regulatory complex (Viswakarma et al. 2010). It could regulate the expression of several target genes

involved in mitochondrial dysfunction, oxidative stress, proteasomal dysfunction, autophagy, neuroinflammation, and apoptosis lead to neuronal survival and neuroprotection (Katsouri et al. 2016).

PGC-1 $\alpha$  is a metabolic co-activator contributes in the glucose, lipid, and energy metabolism, also promotes mitochondrial biogenesis and exhibits neuroprotective effects against several neurodegenerative diseases (Róna-Vörös and Weydt 2010). The reports implicated that expressions of PGC-1 $\alpha$  were remarkably decreased in the Alzheimer's disease brain (Qin et al. 2009) and up-regulation of PGC-1 $\alpha$  protected the neurons against amyloid  $\beta_{1-42}$ -induced neurotoxicity (Zhu et al. 2012; Katsouri et al. 2011). Impairment of the PGC-1 $\alpha$  triggers the degeneration of neurons by mitochondrial dysfunction (Johri et al. 2013) and induction of PGC-1 $\alpha$  regulates the gene expression of several ROS enzymes such as superoxide dismutase 1 and 2, catalase, and glutathione peroxidase-1 which decreasing oxidative stress and increasing mitochondrial biosynthesis resulted in neuroprotection (St-Pierre et al. 2006). In this context, stimulation of PGC-1 $\alpha$  signaling through activation of PPAR- $\gamma$  receptors could be a promising strategy for neuroprotection in neurodegenerative conditions (Hunter and Bing 2007).

Hence, we proposed to design and synthesize few glitazones as novel glitazars which could activate the PPAR- $\gamma$ -dependent PGC-1 $\alpha$  signaling in neurons that may have more therapeutic impact on neurodegenerative disorders. In the present study, structurally diverse two novel glitazones were designed using in-silico ligand-based drug design methods. Then binding affinity and interaction analysis of designed glitazones with PPAR- $\gamma$  were performed through docking studies. The compounds were subjected to molecular dynamics study using leapfrog verlet dynamics integrator to find out the energy parameters such as potential energy, kinetic energy, and conformational changes of the docked protein-ligand complexes (PPAR- $\gamma$  and PGC-1 $\alpha$ ). The designed glitazones were synthesized using appropriate synthetic schemes and the synthesized glitazones were purified and analyzed to confirm their molecular structures. Thereafter, compounds were subjected to preliminary neuroprotective analysis in lipopolysaccharide (LPS) intoxicated SH-SY5Y neuroblastoma cell lines. The neuroprotective activity was assessed by performing cell viability assay, plotting dose response curve of test glitazones vs standard glitazone and morphological observation in LPS-intoxicated SH-SY5Y cell lines. The pathophysiological parameters during neuroinflammation such as pro-inflammatory cytokines (TNF- $\alpha$ , IL-1 $\beta$ ) and ROS-like lipid peroxide (LPO) and nitric oxide (NO) were estimated to assess the level of anti-neuroinflammatory and free radical scavenging potential of novel glitazones in LPS-mediated neuroinflammatory conditions.

## Materials and Methods

### Rational Design of Glitazones for PGC-1 $\alpha$ Activation via PPAR- $\gamma$ Binding Using Molecular Docking

Docking is a lock and key method; it can be executed with various algorithms. CDOCKER algorithm is basically a simulated annealing-based docking that utilizes CHARMM force field for simulation (Ewing et al. 2001, Wu et al. 2003a, b). Prior to docking, three-dimensional (3D) structure of the protein (PDB ID-3CS8) (Li et al. 2008) was downloaded from Structural database PDB (<http://www.rcsb.org>). The X-ray crystal structure of PPAR- $\gamma$  bound to PGC-1 $\alpha$  having 2.3 Å resolution was processed using prepared protein protocol to make sure that side chain, loops region, and other conformers were removed. It was also ought to be free from water molecules because in this case there is no role of water molecule to bridge the connection between ligand and active site. Subsequently, ligands were prepared to remove the duplicates and to fix its chemical valences. The prepared protein and ligands were subjected to docking. The binding site of the protein was identified through receptor cavity tool using site search and flood filling algorithm. The site-1 had the volume of 1065 Å<sup>3</sup> and a point count of 8520 in equal grid spacing of 0.5(X), 0.5(Y), and 0.5(Z) directions, respectively. The compounds Glitazone 1 (**G1**), Glitazone 2 (**G2**), and standard rosiglitazone were docked with the defined sphere site of 22.91(X), 2.019(Y), and 25.46(Z) using random conformations with 1000 steps of dynamics with default simulation annealing. The final best pose results were taken for interaction analysis and molecular dynamics (the PPAR- $\gamma$  bound to PGC-1 $\alpha$  and **G1** docked complex in the form of pdb file is available as supporting information).

### Molecular Dynamics and Simulation

The best pose of a compound having maximum favorable bonded interaction with protein and dock score was subjected to 1000 ps dynamics with leapfrog verlet dynamics integrator (Tuckerman et al. 1992). In this study, apo-protein (PPAR- $\gamma$  with PGC-1 $\alpha$ ) and other three receptor-ligand interaction complexes such as PPAR- $\gamma$  with PGC-1 $\alpha$  and compound **G1**; PPAR- $\gamma$  with PGC-1 $\alpha$  and compound **G2**; and PPAR- $\gamma$  with PGC-1 $\alpha$  and standard rosiglitazone were considered. Initially, complexes and apo-protein were geometrically optimized using popular minimization techniques steepest descent and conjugate gradient for 1000 steps individually. Consequently, all the samples were gradually simulated and heated for a temperature of 50 K followed by its ramping to 300 K and then equilibrated by 100 steps at 300 K for even distribution of atoms in the system. At last, dynamics production was processed for 1000 ps using CHARMM (Vanommeslaeghe et al. 2010; Skeel et al. 1997).

Additionally, SHAKE algorithm was introduced to fix all bond and angle constraints during the simulation process. Finally, energy parameters such as potential energy, kinetic energy, and conformational changes of the complexes and apo-protein were studied (the PPAR- $\gamma$  bound to PGC-1 $\alpha$  and rosiglitazone dynamics simulation movie is available as supporting information).

### Synthesis and Characterization

Synthetic work was done by procuring available laboratory-grade reagents and analytical grade solvents, Thin layer chromatography (TLC) was performed to monitor the reactions, and all the reported compounds were purified by column chromatography. Infrared (IR) spectra of compounds were recorded on Shimadzu FT-IR 8400-S spectrophotometer by KBr pellet technique and are expressed in cm<sup>-1</sup>. <sup>1</sup>H-NMR and <sup>13</sup>C-NMR spectra were recorded on Bruker 400 MHz FT-NMR spectrophotometer using DMSO D<sub>6</sub> and CDCl<sub>3</sub> as the solvents and TMS as internal standard ( $\delta$  ppm). Mass spectra were obtained using LC-MS ACQUITY UPLC mass spectrometer under ES ionization at 70 eV and time of flight detector. Retention time (RT) was also observed on the same UPLC instrument under optimized chromatographic conditions; Column: C<sub>18</sub> 1.7 micron, flow rate 0.4 ml/min, run time 15 min, injection volume 10  $\mu$ L, Detector: PDA Detector, TOF, Elution: Gradient, Mobile phase: 0.1% FA in water and Acetonitrile, Column temperature 60 °C.

### General Procedure for the Synthesis of Sodium Salt of Vanillin and *p*-Hydroxy Benzaldehyde

Sodium salt of vanillin and *p*-hydroxy benzaldehyde was prepared by mixing 0.02 M equivalents of vanillin or *p*-hydroxy benzaldehyde in 20 ml of water in a beaker with 0.02 M sodium hydroxide and the solution was mechanically stirred at room temperature until whole solution became clear (Bala et al. 2010).

### General Procedure for Linking Sodium Salts of Vanillin and *p*-Hydroxy Benzaldehyde with Chloroacetic Acid

It was prepared by modifying Williamson's ether synthesis protocol as described in Zubrys and Siebenmann 1954. The prepared solution of sodium salt of vanillin and *p*-hydroxy benzaldehyde was taken in a beaker, to that, 30 ml of chloroform was added and the solution was stirred for a period of 10 min at room temperature. To the above solution, 0.02 M chloroacetic acid crystals dissolved in 15 ml of distilled water and 0.02 M sodium hydroxide pellets dissolved in 15 ml of distilled water were added. The reaction mixture was continued to stir for another 10 min. The resultant mixture was allowed to settle, then the whole mixture was poured into a

separating funnel and the aqueous layer was taken in a round bottom flask, and the solution was refluxed with stirring at a temperature of 120–140 °C for 3 h. Reaction mixture was allowed to cool and concentrated HCl was added dropwise until the precipitation ceases, filtered, and 20 ml of chloroform was added and suspended in a separating funnel. To this mixture, saturated solution of sodium bicarbonate was added until whole precipitate goes into the aqueous phase. Sequentially, aqueous phase was acidified with concentrated HCl to precipitate out the product.

#### 2-(4-formylphenoxy) acetic acid (1)

Pale brown solid, yield 75%, mp 185–187 °C. IR (KBr,  $\text{cm}^{-1}$ ): 3448.84 (O-H, Acid), 3069.00 (Ar C-H), 1759.14 (C=O, Acid), 1651.12 (C=O, Aldehyde), 1427.37 (C-C), 1226.77 (C-O).  $^1\text{H}$  NMR ( $\delta$  ppm,  $\text{CDCl}_3$ ): 4.487 (s, 2H,  $\text{CH}_2$ ), 6.837–7.655 (m, 4H, ArH), 9.694 (s, 1H, CHO). MS (m/z): M+1 peak found 181.0835, (M+1 peak calculated 181.16). Mass fragments (m/z): 181.0835, 182.0845. HPLC (RT) 3.19 min.

#### 2-(4-formyl-2-methoxyphenoxy) acetic acid (2)

Off white solid, yield 60%, mp 145–147 °C. IR (KBr,  $\text{cm}^{-1}$ ): 3510.56 (O-H, Acid), 3091.99 (ArC-H), 1766.85 (C=O, Acid), 1643.41 (C=O, Aldehyde), 1411.94 (C-C), 1273.06 (C-O).  $^1\text{H}$  NMR ( $\delta$  ppm,  $\text{CDCl}_3$ ): 3.849 (s, 3H,  $\text{OCH}_3$ ), 4.656 (s, 2H,  $\text{CH}_2$ ), 6.814–7.347 (m, 3H, ArH), 9.758 (s, 1H, CHO). MS (m/z): M+1 peak found 211.0897, (M+1 peak calculated 211.05). Mass fragments (m/z): 211.0897, 212.0941. HPLC (RT): 3.33 min.

### General Procedure for the Synthesis of Schiff Base

The imine (-CH=N-) linkage between an amine and aldehyde was done by reacting equivalent quantities of arylamine and aldehyde in the presence of catalytic amount of glacial acetic acid, stirred without heating according to the procedure reported by Hugo Schiff (1864) (Shah and Baseer 2012). Equimolar quantities of formylphenoxyacetic acid and substituted aromatic amine were dissolved in absolute ethanol and mixed together, to that, few drops of glacial acetic acid and few activated molecular sieves were added and finally stirred for 8–12 h. The reaction was monitored from time to time. The formed precipitate was filtered, washed with minimal quantities of cold aqueous ethanol, and purified by column chromatography using 25% ethyl acetate in pet ether as mobile phase.

#### 2-(2-methoxy-4-((E)-(pyridin-2-ylimino)methyl)phenoxy)acetic acid (G1)

White amorphous solid, yield 80%, mp 187–189 °C. IR (KBr,  $\text{cm}^{-1}$ ): 3425.69 (O-H, Acid), 3078.20 (Ar-H), 1690.55 (C=O, Acid), 1604.83 (C=N, Imine), 1273.06 (C-N), 1218.05 (C-O).  $^1\text{H}$  NMR ( $\delta$  ppm,  $\text{CDCl}_3$ ): 3.817 (s, 3H,  $\text{OCH}_3$ ), 4.404 (s, 2H,  $\text{CH}_2$ ), 6.419–6.433 (d, 2H, ArH), 6.921 (m, 1H, ArH), 7.258–7.330 (d, 2H, ArH), 7.652 (m, 1H, ArH), 8.122 (d, 1H, ArH), 9.124 (s, 1H, CH=N).  $^{13}\text{C}$  NMR: ( $\delta$  ppm,  $\text{CDCl}_3$ ):

55.999, 65.826, 110.342, 112.990, 115.335, 122.620, 123.599, 130.231, 144.764, 149.507, 150.546, 157.338, 158.218, 164.489, 172.386. MS (m/z): M+1 peak found 287.4666, (M+1 peak calculated 287.10). Mass fragments (m/z): 287.4666, 278.4613, 271.9437. HPLC (RT): 0.50 min.

#### 2-(4-((1E)-(2-(2,4-dinitrophenyl)hydrazin-1-ylidene)methyl)phenoxy)acetic acid (G2)

Orange amorphous solid, yield 82%, mp 193–195 °C. IR (KBr,  $\text{cm}^{-1}$ ): 3618.58 (N-H), 3294.53 (O-H, Acid), 3109.35 (Ar-H), 1728.28 (C=O, Acid), 1604.83 (C=N, Imine), 1504.53 ( $\text{NO}_2$ ), 1334.78 (C-N), 1257.63 (C-O).  $^1\text{H}$  NMR ( $\delta$  ppm,  $\text{DMSO } D_6$ ): 4.552 (s, 2H,  $\text{CH}_2$ ), 6.870–6.893 (d, 2H, ArH), 7.613–7.635 (d, 2H, ArH), 7.976–8.000 (d, 1H, ArH), 8.196 (s, 1H, CH=N), 8.203–8.226 (m, 1H, ArH), 8.956 (s, 1H, ArH), 11.327 (s, 1H, NH).  $^{13}\text{C}$  NMR: ( $\delta$  ppm,  $\text{DMSO } D_6$ ): 65.037, 77.460, 77.786, 77.983, 78.105, 115.047, 116.891, 123.311, 126.983, 129.108, 129.268, 129.662, 144.916, 148.550, 160.062, 170.155. MS (m/z): M+1 peak found 361.1061, (M+1 peak calculated 361.07). Mass fragments (m/z): 361.1061, 351.1051, 349.2133. HPLC (RT): 8.56 min.

### In Vitro Neuroprotective Evaluation of Novel Glitazones in LPS Intoxicated SH-SY5Y Cell Lines

#### Cell Culture, $\text{IC}_{50}$ , and $\text{EC}_{50}$ Determination of Synthesized Glitazones

SH-SY5Y human neuroblastoma cells were obtained from National Centre for Cell Science (NCCS), Pune, India and maintained as per the standard protocol in Minimum Essential Medium (MEM) supplemented with 10% fetal bovine serum (FBS), amphotericin (3  $\mu\text{g}/\text{ml}$ ), gentamycin (400  $\mu\text{g}/\text{ml}$ ), streptomycin (250  $\mu\text{g}/\text{ml}$ ), and penicillin (250 units/ml) in a carbon dioxide incubator at 5%  $\text{CO}_2$ . The neuronal viability in terms of mitochondrial metabolic function was evaluated by MTT [(3-[4,5-dimethylthiazol-2-yl]-2,5 diphenyl tetrazolium bromide)] assay based on the principle involving reduction of MTT to formazan. To find the cytotoxicity of the compounds, SH-SY5Y cells were incubated with seven different doses of novel glitazones between 1.953125 and 125  $\mu\text{g}/\text{ml}$  for 24 h. Then SH-SY5Y cells were washed with phosphate-buffered saline (PBS) and incubated with MTT (5 mg/ml) in PBS for 3 h at 37 °C in 5%  $\text{CO}_2$ . After further washing, the formazan crystals were dissolved with isopropanol and the absorbance was measured at 570 nm. The standard formula was applied to calculate the % cytotoxicity of the novel glitazones in SH-SY5Y cells and  $\text{IC}_{50}$  value was calculated for further assays (Kaja et al. 2011). To assess the protective effect, the SH-SY5Y cells were pre-treated with eight different doses of novel glitazones between 1.953125 and 250 nM and each group was incubated with LPS 10 ng/ml for 24 h. The same procedure was carried out as above

and percentage viability of cells was calculated in terms of percentage neuroprotection. Then the dose response curve of new compounds vs known glitazones was plotted using Graph Pad Prism software. The above different doses of compounds were converted to Log dose and the dose response curve was plotted with Log dose vs % protection to find out the EC<sub>50</sub> value to compare the protective efficacy between test compounds and standard Pioglitazone.

### Drug Pre-treatment and LPS Intoxication

The SH-SY5Y cell lines were maintained as per the standard protocol in Minimum Essential Medium (MEM). 5000–10,000 cells/well were seeded in 96 well plates and the viability was tested using trypan blue dye with the help of a hemocytometer and 95% of viability was confirmed. The cells were then pre-treated with synthesized glitazones and standard pioglitazone at IC<sub>50</sub> dose. After 24 h of treatment with respective drugs, all the cells were incubated with LPS (10 ng/ml) to induce the inflammation. After 24 h of LPS incubation, the following evaluations were performed.

### Cell Morphological Observation

The morphological changes in the SH-SY5Y cell lines after respective treatments were observed by using phase contrast microscopy (Motic).

### Preparation of Cell Lysates

After the study period, the medium was aspirated and cells were washed with the ice-cold phosphate buffer saline, scraped, and were centrifuged at 5000 rpm for 5 min at 4 °C. The cell pellets were resuspended in 2000 µl of lysis buffer (10 mM Tris-HCl, pH 7.5, 50 mM NaCl, 1% Triton X-100, 5 mM EDTA, 50 mM NaF, 100 µM Na<sub>3</sub>VO<sub>4</sub>, 1 mM PMSF, 10 µg/ml leupeptin, and 10 µg/ml aprotinin) and incubated on ice for 30 min. The cell lysates were obtained by centrifugation at 12,000 rpm for 20 min at 4 °C. Cell lysates obtained were stored at – 20 °C until use.

### Measurement of IL-1β & TNF-α (Pro-inflammatory Cytokines) by ELISA

The levels of IL-1β and TNF-α were assessed in cell lysates using respective ELISA kits (Invitrogen, R&D systems & Alpha diagnostics, USA) as per the manufacturer's protocol. Briefly, 150 µl distilled water was added to the standard and blank wells for standard calibration and 100 µl distilled water and 50 µl of each supernatant were added in duplicate into the wells. After incubation for 3 h at room temperature, the wells were emptied and washed three times with 150 µl of wash buffer. TMB substrate (100 µl) was added to each well and

incubated for 15 min at room temperature, followed by addition of 100 µl stop-solution to all wells including blank wells. The absorbance was determined at 410 nm using above-mentioned ELISA reader (Roeske-Nielsen et al. 2004).

### Lipid Peroxide (LPO) Assay

Lipid peroxidation was evaluated in cell lysates by measuring the malondialdehyde content according to the TBA test described by Ohkawa et al. (1979) with slight modification. 0.2 ml of the cell lysate was taken and to this, 0.8 ml saline, 0.5 ml of BHT, and 3.5 ml TBA reagent (0.8%) were added and incubated at 60 °C. After cooling, the solution was centrifuged at 2000 rpm for 10 min. The absorbance of the supernatant was determined at 532 nm using spectrophotometer against the blank.

### Nitric Oxide (NO) Assay

Nitric oxide was assayed by taking 0.2 ml of medium followed by the addition of 1.8 ml of saline and 0.4 ml of 35% sulphosalicylic acid (SSA) for protein precipitation. The precipitate was removed by centrifugation at 4000 rpm for 10 min. To 1 ml of aliquot of supernatant, 2 ml Griess reagent (1 g of sulphanilamide dissolved in small volume of water, 2 ml of orthophosphoric acid and 100 mg of naphthyl ethyl diamine were added and the final volume was made up to 100 ml with distilled water). The mixture was allowed to stand for 20 min under dark conditions. The color intensity of the chromogen was read at 540 nm. The standard calibration curve was plotted using sodium nitrite in the concentration range 200–1000 ng (Green et al. 1982).

## Results and Discussion

### Rational Design of Glitazones

Thiazolidinediones (TZDs), a class of glitazone family are widely used as insulin sensitizers due to their characteristic PPAR-γ agonism. Since PPAR-γ receptors are bound to PGC-1α domain; the efforts are put forth to design novel PPAR-γ agonists that can cause conformational changes in the PPAR-γ and co-activators especially PGC-1α binding domain. The rationale here is, the conformational changes at PGC-1α binding domain may up-regulate the mitochondrial biogenesis process thereby offer advantage in the treatment of neurodegenerative disorders. In this context, the structures of glitazones are contrived to meet the pharmacotherapeutic requirements. Based on bioisostere principle, the structural features necessary for glitazone to interact with PPAR-γ receptors such as acidic head group, aromatic trunk, heteroatom spacer, and finally lipophilic tail were modified to build novel

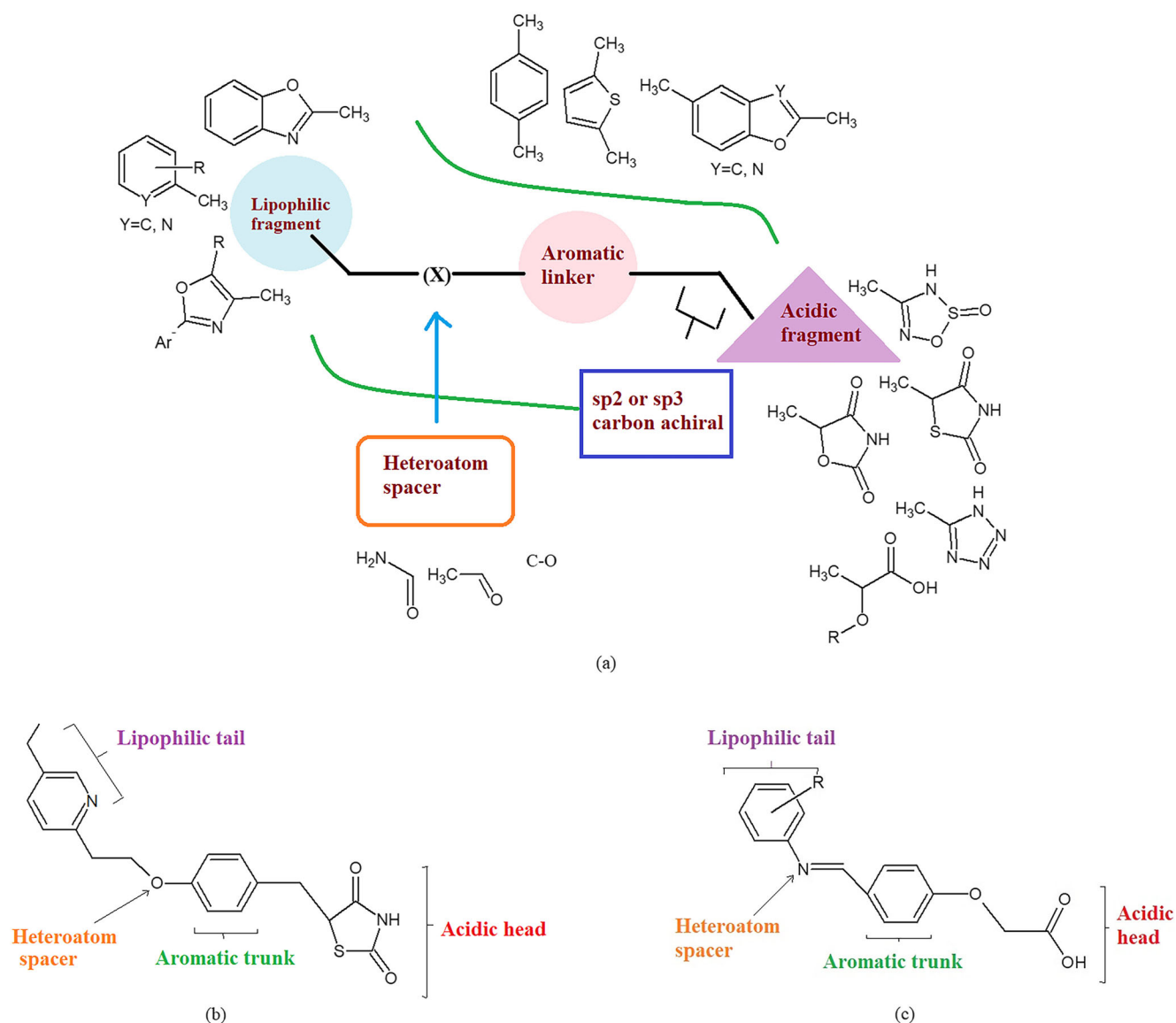
glitazones (Kulkarni et al. 1999). Phenoxy acetic acid constituted acidic head instead of thiazolidinedione, substituted benzene constituted trunk, and imine linkage constituted two carbon linker followed by pyridine and its isostere benzene as lipophilic tail as shown in (Fig. 1a–c).

## Chemistry and Synthesis

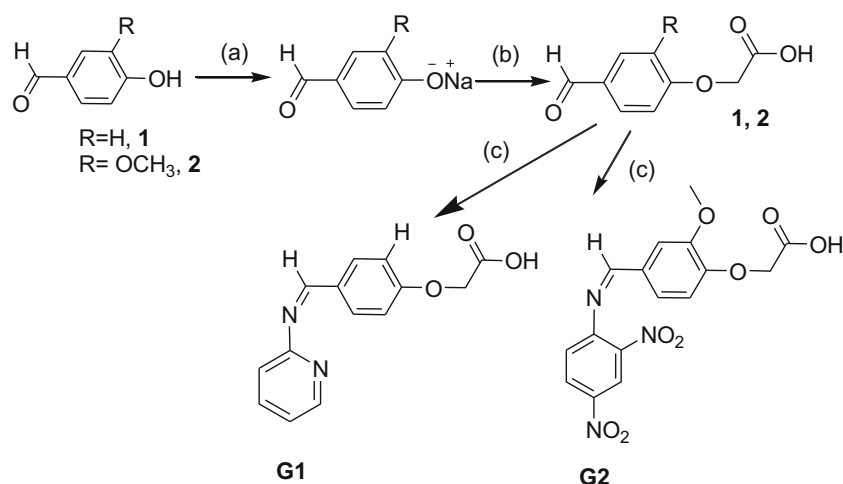
Rationally designed compounds were synthesized according to the scheme described in Fig. 2 (Zubrys and Siebenmann 1954; Shah and Baseer 2012). Two aromatic aldehydes, viz. 4-hydroxy benzaldehyde and 4-hydroxy-3-methoxy benzaldehyde (vanillin) are selected as building blocks. Initially, the hydroxyl group of aldehydes was converted to corresponding phenoxy-acetic acids by adopting the modified Williamson's ether synthesis. Further, the formed intermediate

was connected to the lipophilic tail by condensation with 2-amino pyridine (compound **G1**) and 2,4-dinitro phenylhydrazine (compound **G2**) using absolute alcohol as solvent in the presence of catalytic amount of acetic acid and activated molecular sieves to form Schiff's base imine linkage. The products were purified by column chromatography using ethyl acetate and n-hexane as mobile phase by gradient elution technique. The method adopted to synthesize the final product was very feasible and facile. The two synthesized Schiff's bases were checked for their possible aqueous hydrolysis of imine linkage. However, both the Schiff's bases were found to stable in water when studied for 48 h.

The structures of the synthesized glitazones confirmed via IR, NMR, and Mass spectral interpretation. The appearance of characteristic peak in the range of  $1580.50\text{--}1604.90\text{ cm}^{-1}$  in all IR spectra along with the absence of NH stretch proved the



**Fig. 1** a General structural features of glitazones or TZDs. b Structural features of pioglitazone. c Structural features of designed glitazones

**Fig. 2** Synthetic scheme of glitazones

formation of imine bond (CH=N). All the compounds showed characteristic C=O stretching of the carboxyl group in the range of 1650.42–1743.35  $\text{cm}^{-1}$  along with O-H stretching in the range of 3200.25–3400.23  $\text{cm}^{-1}$ . From  $^1\text{H-NMR}$  spectra it is observed that methylene protons ( $\text{CH}_2$ ), which are bridge between phenoxy and carboxylic acid moiety appeared as singlet in the range of  $\delta$  4.45 to  $\delta$  4.68 ppm and proton attached to imine linkage ( $\text{H-C=N}$ ) of Schiff base has resonated between  $\delta$  8.23 and  $\delta$  8.98 ppm which in turn confirmed the formation of imine. It is very interesting to notice that the compounds **G1** and **G2** showed,  $-\text{CH}$  signal for imine ( $-\text{CH=N}$ ) at  $\delta$  ppm 8.9, that indicates the  $-\text{CH=N}$  linkage is of 'E' configuration.

**Reagents and Condition** (a) NaOH,  $\text{H}_2\text{O}$ , stir. (b)  $\text{ClCH}_2\text{COOH}$ , NaOH,  $\text{H}_2\text{O}$  reflux at 120–140  $^\circ\text{C}$  for 3 h. (c) Aromatic amine, gl. acetic acid, absolute ethanol, molecular sieves, reflux with stirring for 8–12 h.

### Binding Affinity and Interaction Analysis Through Docking with PPAR- $\gamma$

The main objective of the molecular docking study was to elucidate binding interactions between agonists/glitazones and PPAR- $\gamma$  receptor and also to identify conformational changes towards the PGC-1 $\alpha$  domain. There are various algorithms existing for docking, one such best tool used for docking via discovery studio is CDOCKER because it uses CHARMM-based molecular dynamics (MD) scheme to dock

ligands into a receptor binding site (Wu et al. 2003a, b). In order to validate the tool effectiveness, the native ligand and the standard drug rosiglitazone re-docking study indicates that the tool predicts the reliable results. The molecular docking results provided significant information about the -CDOCKER energy, -CDOCKER interaction energy, and binding orientation of receptor-ligand interactions. The docking results are summarized in Table 1. It has been found that **G1**, **G2**, and rosiglitazone bound to the same active site as reported in the RCSB crystallographic data. The standard drug rosiglitazone showed docking and interaction energy of 32.3167 kcal/mol and 39.6259 kcal/mol, respectively. The binding accuracy of reference standard, rosiglitazone was validated by redocking with an RMSD value of 0.909  $\text{A}^\circ$ . The binding interactions include one hydrogen bond with Tyr473 and several hydrophobic contacts with Ile281, Cys285, Ile326, Ile341, Met348, Met364, and His449 from arm-I and arm-II of the LBD of PPAR- $\gamma$ . Thus, possibly any PPAR- $\gamma$  binding with His323, Tyr327, His449, and Tyr473 from arm-I of the LBD of PPAR- $\gamma$  has transactivation activity (Cardin et al. 2012). Similarly, Compound **G1** and Compound **G2** have shown docking and interaction energy of 16.1183 kcal/mol, 23.4904 kcal/mol and 45.1763 kcal/mol, 32.6616 kcal/mol, respectively. The common interacting amino acid with hydrogen and hydrophobic interaction with arm-I, arm-II, and arm-III or entrance (E) residues like Ile281, Cys285, Arg288, Leu330, Ile341, Met348, Met364, and Lys261 are shown in Fig. 3A–C. These interactions are typical for PPAR- $\gamma$  partial agonists (Guasch et al. 2012).

**Table 1** CDOCKER Score for the respective ligand protein interaction

Compounds	CDOCKER energy (kcal/mol)	CDOCKER interaction energy (kcal/mol)
Glitazone 1 ( <b>G1</b> )	– 16.1183	– 45.1763
Glitazone 2 ( <b>G2</b> )	– 23.4904	– 32.6616
Standard-rosiglitazone	– 32.3167	– 39.6259

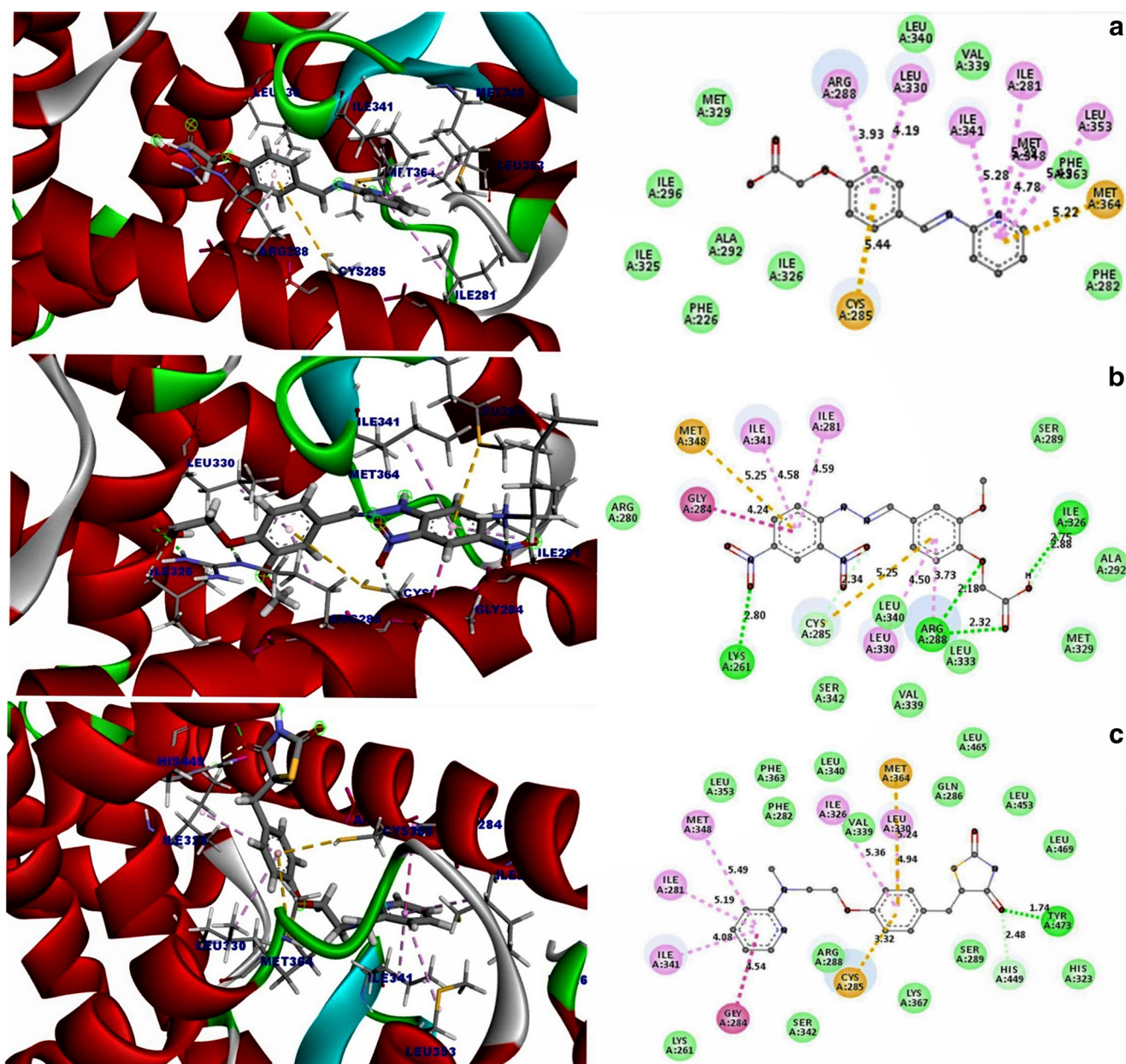


**Fig. 3** A 3D and 2D representation of Compound G1. B 3D and 2D representation of Compound G2. C 3D and 2D representation of standard drug rosiglitazone

### Activation and Molecular Mechanism of PPAR- $\gamma$ with PGC-1 $\alpha$

The peroxisome proliferator-activated receptor gamma (PPAR- $\gamma$ ) belongs to the nuclear hormone receptor superfamily. They are broadly involved in the regulation of genes for various physiological processes such as inflammation, glucose metabolism, cellular differentiation and proliferation, and lipid homeostasis (Delerive et al. 2001). Many studies have reported peroxisome proliferator-activated receptor gamma (PPAR) co-activator (PGC-1 $\alpha$ ) as a crucial potential therapeutic target for neurological dysfunction (Corona and

Duchen 2015). Apparently, the function of PPAR- $\gamma$  agonist with PGC-1 $\alpha$  was addressed as a neuroprotectant in neurodegenerative disorders like Parkinson disease (PD) and Alzheimer's disease (Zheng et al. 2010; Jin et al. 2013) to support the statement, administration of TZDs increases the PGC-1 $\alpha$  responsive genes and blocked the loss of dopaminergic regions (Zheng et al. 2010). But the molecular level mechanism and the activation of the PGC-1 $\alpha$  upon binding of PPAR- $\gamma$  agonist and its atomic level interaction were not clearly reported.

This study is focused only on the role of how the conformational changes in the secondary structure of the protein

activate the PGC-1 $\alpha$ . Previously, it was reported that TZDs bound PPAR- $\gamma$  ligand-binding domain (LBD) has a strong binding affinity with various LXXLL motif co-activator (Li et al. 2008). In order to identify the structural contribution of the PPAR- $\gamma$  agonist in the ligand-binding domain (LBD) molecular docking was initially processed followed by Monte Carlo simulation using CHARMM force field. The outcome has revealed that structure has undergone various conformational changes at helix and coil region. To support the argument, the realistic molecular dynamics and simulation were conducted for four different complex apo-proteins (PPAR- $\gamma$  and PGC-1 $\alpha$ ), the best-docked complex of apo-protein with various agonists like **G1**, **G2**, and standard drug.

It was observed that without ligand binding to the LBD of PPAR- $\gamma$ , the structure of the adjacent helix, C-terminal helix and PGC-1 $\alpha$  doesn't show any structural variation. On the other hand, any agonist binding to the PPAR- $\gamma$  LBD such as compound **G1**, compound **G2**, and rosiglitazone shows the

transformation of the secondary structure of the protein. Eventually, 1000 ps dynamics shows Compound **G1** binding to LBD affects the C-terminal helix and it transformed the coil conformation while other helices moderately show changes in secondary structure with the final potential energy of  $-17,687.60$  kcal/mol (Fig. 4C). Moreover, the residue Leu145 of PGC-1 $\alpha$  1D1 forms two direct hydrogen bonds with Asn312 and one hydrogen bond interaction with Asp310. Secondly, Ser142 and Leu143 form direction conventional hydrogen bonding with Gly471 present at C-terminal of PPAR- $\gamma$ . The apo-protein complex energy  $-17,407.10$  kcal/mol forms only one direct hydrogen bond interaction between Leu145-Asn312, no bonding with Ser142 that implies least stability and interaction between the PPAR- $\gamma$  and PGC-1 $\alpha$ , furthermore weak conformation change was observed (Fig. 4A). Similarly, Compound **G2** binding with LBD of PPAR- $\gamma$  had shown changes in intermolecular interactions compared with Compound **G1** and rosiglitazone. Evidently,

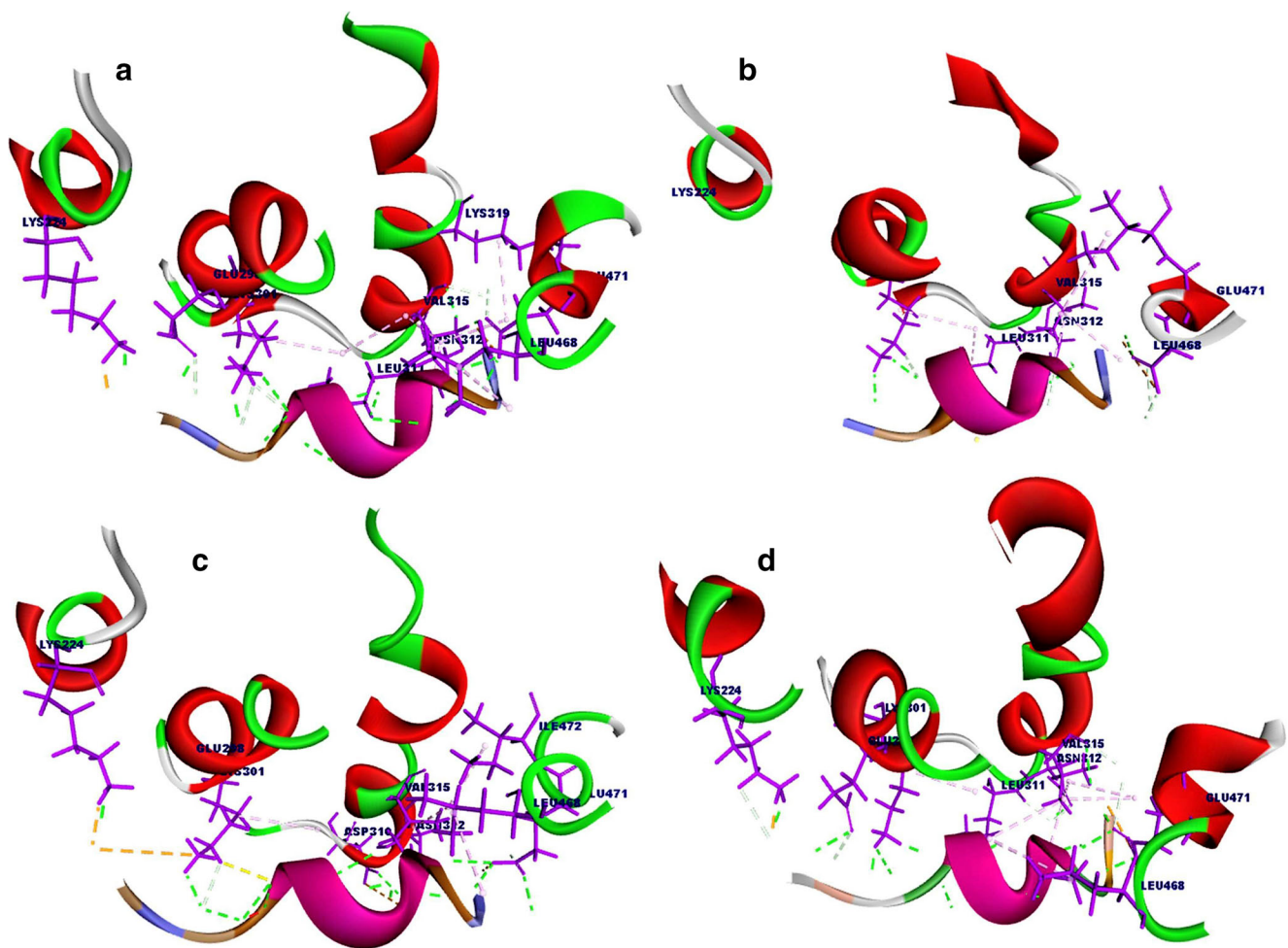


**Fig. 4** Conformational changes and interaction of PPAR- $\gamma$  with PGC-1 $\alpha$ . **A** Apo-protein interaction (PPAR- $\gamma$ -PGC-1 $\alpha$ ). **B** Compound **G2** binding to PPAR- $\gamma$  LBD and its associated conformation changes in PGC-1 $\alpha$ . **C** Compound **G1** binding to PPAR- $\gamma$  LBD and its associated

conformation changes in PGC-1 $\alpha$ . **D** Standard drug rosiglitazone binding to PPAR- $\gamma$  LBD and its associated conformation changes in PGC-1 $\alpha$ . Pink color in the figure is LXXLL motif of PGC-1 $\alpha$

Compound **G2** binding to LDB region affects the binding of A: LYS224: HZ3 - B: ALA152: OCT2(PPAR- $\gamma$ -PGC-1 $\alpha$ ) also the helix region (Asn308–Ile 325) shows more structural deviation and transformation with a final potential energy of  $-17,432.10$  kcal/mol (Fig. 4B). Likewise, standard drug rosiglitazone binding to LDB forms two direct hydrogen bond between residue Leu145 of PGC-1 $\alpha$  and Asn312 of PPAR- $\gamma$  (Li et al. 2008) and conformation changes are observed in PGC-1 $\alpha$  with an energy of  $-17,627$  kcal/mol (Fig. 4D).

All the complexes except apo-protein forms more than seven intermolecular interactions. These intermolecular interactions stabilize the helical structure of the PGC-1 $\alpha$  1D1 motif, thus facilitating the hydrogen and hydrophobic docking of this helix into PPAR- $\gamma$ . Simultaneously, these unique interactions and interface contacts serve as a basis for the high affinity, specific binding of PPAR- $\gamma$ -PGC-1 $\alpha$  1D1 motif. Also, the binding of ligand to the PPAR- $\gamma$  LBD is directly influencing the conformational changes of PGC-1 $\alpha$  1D1 motif thereby transcripts the various downstream genes involved in mitochondrial biogenesis and antioxidant defenses. In this context, it is evident that PPAR- $\gamma$  agonists have great influence on PGC-1 $\alpha$  activation. Thus, compound **G1** shows equal in energy and binding as like as rosiglitazone even though with 50% of docking score. Perhaps, Compound **G2** with 72% of dock score with energy of  $-17,432.10$  kcal/mol can serve as a better drug candidate. From this, it was clearly stated that only the strong influential binding of drug to the LBD pocket will influence the structural changes, thereby it activates the PGC-1 $\alpha$ . Also, PGC-1 $\alpha$  and PPAR- $\gamma$  agonists regulate the expression of several target genes involved in neuroprotection by suppressing neuroinflammation, mitochondrial dysfunction, and proteasomal dysfunction.

### Neuroprotective Evaluation of Synthesized Glitazones in LPS-intoxicated SH-SY5Y Neuroblastoma Cell Lines

The synthesized novel synthesized glitazones **G1** & **G2** were subjected to preliminary in vitro neuroprotective activity against LPS-induced inflammatory events in SH-SY5Y neuroblastoma cell lines. The neuroprotective activity was assessed by performing cell viability assay, morphological observation and measuring the intracellular pro-inflammatory cytokines TNF- $\alpha$ , IL-1 $\beta$  using ELISA. Additionally, LPO and NO assay were carried out to assess the level of free radical scavenging properties of novel glitazones. The neuroinflammation induced by incubation of SH-SY5Y cell lines with LPS (10 ng/ml) in minimum essential medium at 37 °C for 24 h is one of the standard protocols. In our laboratory, it has been observed that 24 h incubation with 10 ng/ml of LPS is sufficient to stimulate inflammatory reactions. The previous report suggests that LPS-treated neuronal cell lines serve as a good in vitro model mimicking the

**Table 2** The IC<sub>50</sub> value of synthesized glitazones in SH-SY5Y neuroblastoma cell lines

S. no.	Compound name	IC <sub>50</sub> $\mu$ g/ml	EC <sub>50</sub> <sup>a</sup> nM
1	Glitazone 1 ( <b>G1</b> )	53.46 $\pm$ 3.81	46.04 $\pm$ 4.10
2	Glitazone 2 ( <b>G2</b> )	86.65 $\pm$ 6.11	47.88 $\pm$ 2.60
3	Standard-Pioglitazone (P)	45.95 $\pm$ 3.98	> 250 <sup>b</sup>

<sup>a</sup> EC<sub>50</sub> was measured in the presence of LPS 10 ng/ml

<sup>b</sup> Pioglitazone exhibited a maximum neuroprotection of 44.78  $\pm$  1.51 % at 62.5 nM

neuroinflammatory conditions to evaluate the neuroprotective activity of several agents (Rampe et al. 2004).

### Effect of Glitazones on Cell Viability Assay in LPS-intoxicated SH-SY5Y Cell Lines

The synthesized novel glitazones were subjected to MTT assay to evaluate the extent of toxicity (IC<sub>50</sub>) and neuroprotective (EC<sub>50</sub>) effects. The test glitazones **G1** and **G2** are less toxic to SH-SY5Y cell lines because **G1** (53.46  $\pm$  3.81) and **G2** (86.65  $\pm$  6.11) have greater IC<sub>50</sub> than Pioglitazone (45.95  $\pm$  3.98). Interestingly, the test compound **G2** has approximately twofold less cytotoxic than standard pioglitazone (Table 2). The IC<sub>50</sub> values of the each compound were taken for further neuroprotective evaluation. The neuroprotection was observed in LPS-induced inflammatory condition in SH-SY5Y cells. The **G1** and **G2** had significant neuroprotective effect at doses 31.25, 62.5, 125, and 250 nM ( $p < 0.001$ ) when compared to standard pioglitazone (Fig. 5). Pioglitazone exhibited

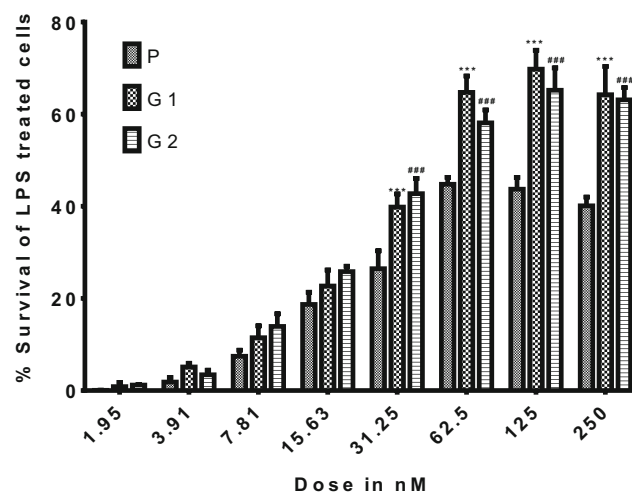


**Fig. 5** Neuroprotective effect of test glitazones and standard pioglitazone in LPS-intoxicated SH-SY5Y cell lines. Statistical significance was determined by one-way ANOVA followed by Dunnett-t test using Graph pad prism Version 5.0. Values are expressed as mean  $\pm$  SEM. Superscript \*\*\* denotes P vs **G1** and ### denotes P vs **G2** at  $p < 0.001$ . P—Pioglitazone, **G1**—Glitazone 1 and **G2**—Glitazone 2

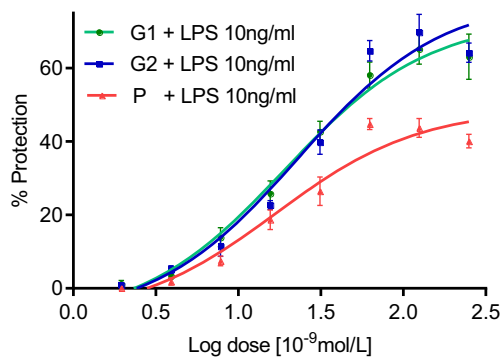
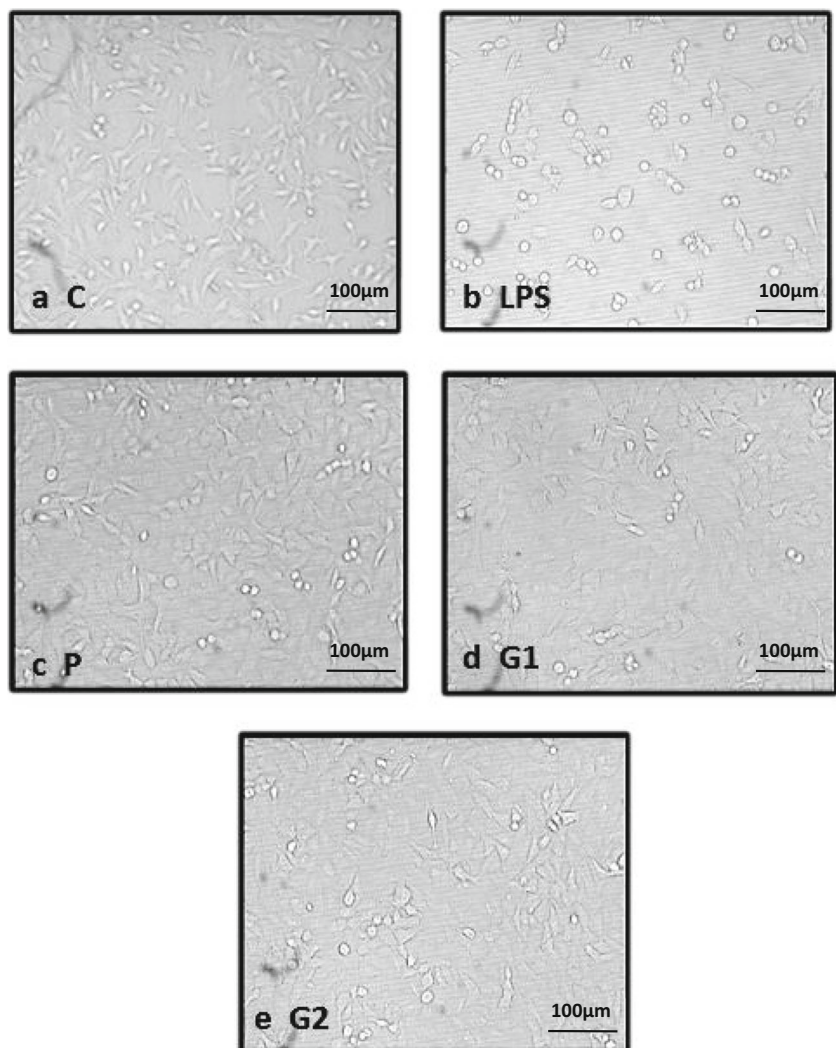


**Fig. 6** Dose response curve of test glitazones vs standard pioglitazone in LPS-intoxicated SH-SY5Y cell lines. Values are expressed as mean  $\pm$  SEM. P—Pioglitazone, G1—Glitazone 1 and G2—Glitazone 2

a maximum of neuroprotection of  $44.78 \pm 1.51$  % at 62.5 nM. After that, at 125 nM ( $43.71 \pm 2.55$ ) and 250 nM there is a decrease in the neuroprotective effect. Pioglitazone did not achieve the 50% neuroprotection in the tested dose in comparison to the test glitazones indicate that the test glitazones are having more neuroprotective efficacy than pioglitazone

**Fig. 7** Effect of novel glitazones on morphological changes in LPS-intoxicated SH-SY5Y cell lines. **a** Control cells. **b** LPS-treated cells. **c** Standard pioglitazone. **d** Glitazone 1. **e** Glitazone 2 treated cells. C—Control, LPS—Lipopolysaccharide, P—Pioglitazone, G1—Glitazone 1 and G2—Glitazone 2

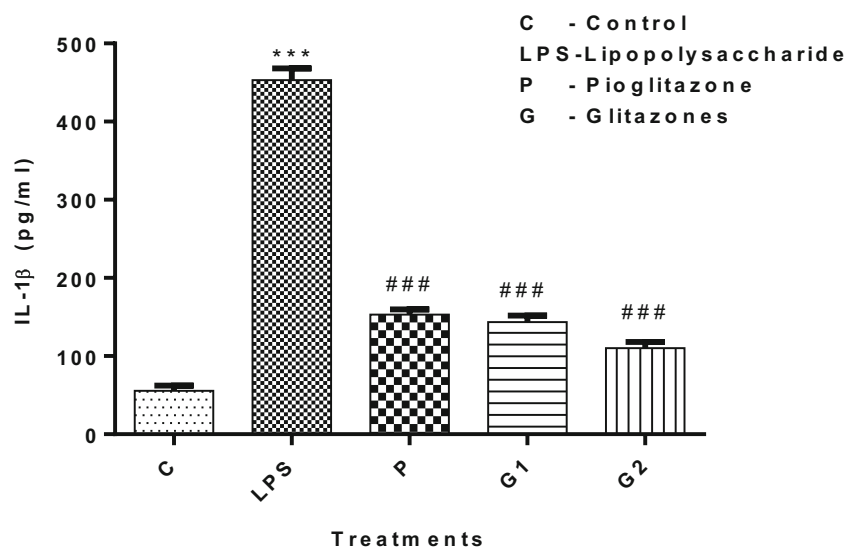


which is further witnessed in dose response curve of test glitazones and standard pioglitazone (Fig. 6). Hence, we could not calculate the  $EC_{50}$  of pioglitazone. The G1 and G2 exhibited a maximum protection of 69.77% and 65.19% at 125 nM. The  $IC_{50}$  and  $EC_{50}$  of synthesized glitazones in SH-SY5Y neuroblastoma cell lines are given in Table 2.

### Effect of Glitazones on Morphological Changes in LPS-intoxicated SH-SY5Y Cell Lines

The control SH-SY5Y cells are small, highly light retractile, fibroblast-like or teardrop-shaped, cells, growing densely and often forming focal accumulations. LPS (10 ng/ml) intoxication caused morphological changes with reduced cell density, swollen, reduced proliferation, and differentiation of cells when compared to the control cells. Pre-treatment with glitazones protected the cells from the LPS toxicity which is evidenced by increased cell density and proliferation. Interestingly, the pre-treatment with G2 has shown remarkable protective effect on LPS-intoxicated SH-SY5Y cells, this

**Fig. 8** Effect of glitazones on IL-1 $\beta$  level in LPS-intoxicated SH-SY5Y cell lines. Statistical significance was determined by one way ANOVA followed by Dunnett-t test using Graph pad prism Version 5.0. Values are expressed as mean  $\pm$  SEM, Superscript \*\*\* denotes  $p < 0.001$  vs control and ### denotes  $p < 0.001$  vs LPS, respectively



effect was comparable with standard pioglitazone which is summarized in Fig. 7a–e.

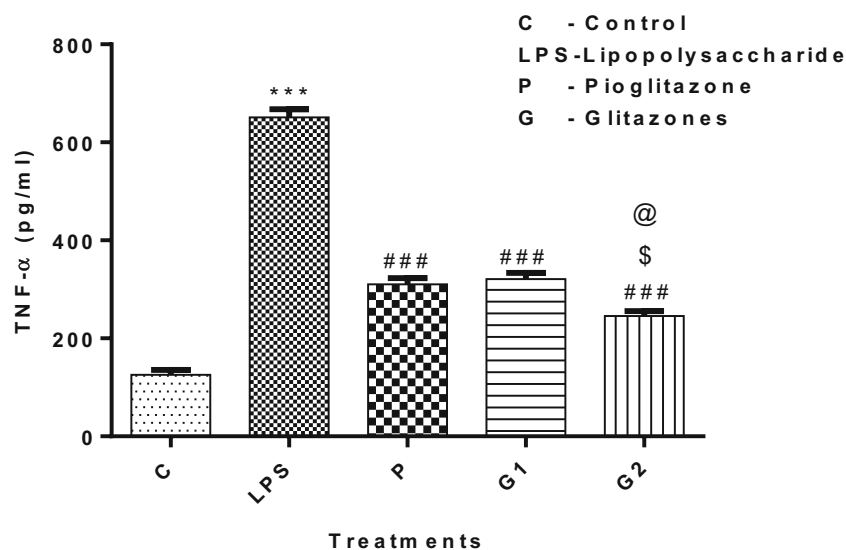
### Effect of Glitazones on Pro-inflammatory Cytokines IL-1 $\beta$ & TNF- $\alpha$ Level in LPS-intoxicated SH-SY5Y Cell Lines

In comparison to control SH-SY5Y cell lines, LPS treatment has significantly ( $p < 0.001$ ) increased the level of IL-1 $\beta$  & TNF- $\alpha$  in LPS-intoxicated SH-SY5Y cell lines which show the extent of inflammatory responses mediated by LPS toxicity. In comparison to LPS-treated group, pre-treatment with pioglitazone, G<sup>1</sup>, and G<sup>2</sup> has remarkably ( $p < 0.001$ ) decreased the level of IL-1 $\beta$  (Fig. 8) & TNF- $\alpha$  (Fig. 9) which indicates the anti-inflammatory potential of novel glitazones. Interestingly, among the two Glitazones, G<sup>2</sup> has shown

significant reduction ( $p < 0.05$ ) of TNF- $\alpha$  level in comparison to Glitazone 1 and standard pioglitazone in LPS-intoxicated cell lines. Thus, the effect of glitazones was found to be similar and comparable with that of the standard pioglitazone in LPS-intoxicated SH-SY5Y cell lines.

The release of IL-1 $\beta$  plays a critical role in the effect of microglial activation on motor neuron viability and IL-1 $\beta$  is among a wide range of factors that up-regulate the expression of COX-2 and the subsequent production of pro-inflammatory cytokines. Previous studies reported that LPS increases the secretions of IL-1 $\beta$  in microglial cells (Arai et al. 2004). The data from the present study shows that glitazones inhibits the level of IL-1 $\beta$  release in LPS-intoxicated SH-SY5Y cells. TNF- $\alpha$  is a potent pro-inflammatory cytokine that plays an important role in neuroinflammation. The present study showed that LPS-stimulation increases TNF- $\alpha$  secretion from

**Fig. 9** Effect of glitazones on TNF- $\alpha$  level in LPS-intoxicated SH-SY5Y cell lines. Statistical significance was determined by one-way ANOVA followed by Dunnett-t test using Graph pad prism Version 5.0. Values are expressed as mean  $\pm$  SEM, Superscript \*\*\* denotes  $p < 0.001$  vs control, ### denotes  $p < 0.001$  vs LPS, \$ denotes  $p < 0.05$  vs P, @ denotes  $p < 0.05$  vs G<sup>1</sup>, respectively



SH-SY5Y cell lines. We further demonstrated that synthetic glitazones significantly downregulated the TNF- $\alpha$  secretion which was triggered by LPS in neuronal cells. **G2** compound exhibited significant effect compared to **G1** and the standard pioglitazone. The results suggest that inhibition of TNF- $\alpha$  secretion from the LPS-intoxicated neuronal cell lines probably participates in the neuroprotective effect of glitazones.

The attenuation of cytokine (IL-1 $\beta$  & TNF- $\alpha$ ) level in LPS-intoxicated SH-SY5Y cell lines endorses the anti-neuroinflammatory activity exhibited by novel glitazones. The mechanism might be attributed through agonist activity at PPAR- $\gamma$  receptors, because earlier report implicates that pioglitazone has decreased the secretion of pro-inflammatory cytokines in astrocytes stimulated with LPS through activation of PPAR- $\gamma$  receptors (Swanson et al. 2011). In addition, previous studies evidence that the stimulation of PPAR- $\gamma$  receptors will recruit/activate its co-activator PGC-1 $\alpha$  which may further suppress the NF- $\kappa$ B expression mediated cytokine release (Qiu and Li 2015). Hence, the novel glitazones evaluated in this study might have ameliorated the IL-1 $\beta$  & TNF- $\alpha$  level through activation of PGC-1 $\alpha$  via PPAR- $\gamma$  agonism which is supported by our in silico molecular interaction study.

### Effect of Glitazones on LPO & NO Levels in LPS-intoxicated SH-SY5Y Cell Lines

Treatment with LPS in SH-SY5Y cell lines have significantly ( $p < 0.001$ ) increased the level of LPO & NO in comparison to control cell lines which indicates the extent of oxidative stress-mediated by LPS toxicity. In comparison to LPS-intoxicated group, pre-treatment with pioglitazone ( $p < 0.001$ ), **G1** ( $p < 0.05$ ), and **G2** ( $p < 0.001$ ) have remarkably decreased the levels of LPO (Fig. 10) & NO (Fig. 11), which indicates the

anti-oxidant potential of pioglitazone and synthesized glitazones. Interestingly, **G2** has shown significant reduction ( $p < 0.05$ ) of NO level than **G1** and pioglitazone, the effect of **G2** is similar and comparable with pioglitazone in LPS-intoxicated SH-SY5Y cell lines.

Earlier study revealed that PGC-1 $\alpha$  is a master regulator of ROS scavenging enzymes and PGC-1 $\alpha$  decreases the oxidative stress by elevating the expression of antioxidant enzymes (Chen et al. 2011). On other hand, downregulation of PGC-1 $\alpha$  results in impairment of antioxidants expression and triggers the reactive oxygen species (ROS) burst and augment the damage to the mitochondrial proteins resulted in neurodegeneration (Marmolino et al. 2010). In the present study, the attenuation of LPO and NO level by glitazones might be attributed through activation of PGC-1 $\alpha$  signaling via PPAR- $\gamma$  receptor activation, because induction of PGC-1 $\alpha$  regulates the gene expression of several reactive oxygen species (ROS) with decreasing oxidative stress and increasing mitochondrial biosynthesis resulted in neuroprotection (St-Pierre et al. 2006).

Previous findings implicate that the neuroinflammation-mediated neurodegeneration play an imperative in the pathogenesis of several neurodegenerative diseases, including Alzheimer's disease (AD), Parkinson's disease (PD), Huntington's disease, multiple sclerosis (MS), and amyotrophic lateral sclerosis (ALS) (Zhao et al. 2019). In the present study, we have incubated potent neuroinflammatory toxin lipopolysaccharide (LPS) in SH-SY5Y cell lines to mimic the inflammatory conditions in the neuronal cell lines. In general, LPS will act on Toll-like receptor-4 (TLR-4) and activate the respective cells to release the pro-inflammatory cytokines such as IL-1 $\alpha$ , IL-1 $\beta$ , IL-6, and TNF- $\alpha$  which are the key mediators of neuroinflammation [Leow-Dyke et al. 2012]. The LPS-mediated cytokine release is predominantly

**Fig. 10** Effect of glitazones on LPO levels in LPS-intoxicated SH-SY5Y cell lines. Statistical significance was determined by one-way ANOVA followed by Dunnett-t test using Graph pad prism Version 5.0. Values are expressed as mean  $\pm$  SEM, Superscript \*\*\* denotes  $p < 0.001$  vs control and ##, ### denotes  $p < 0.01$ ,  $p < 0.001$  vs LPS, respectively

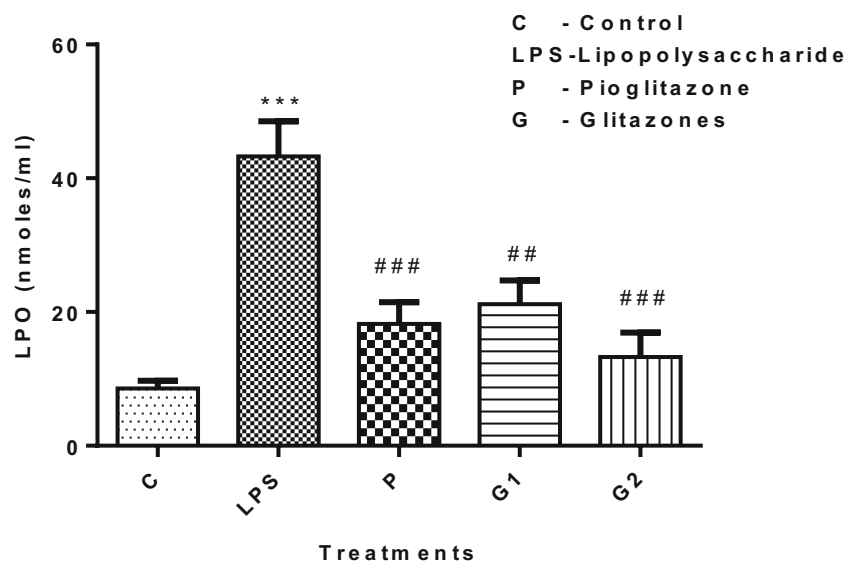
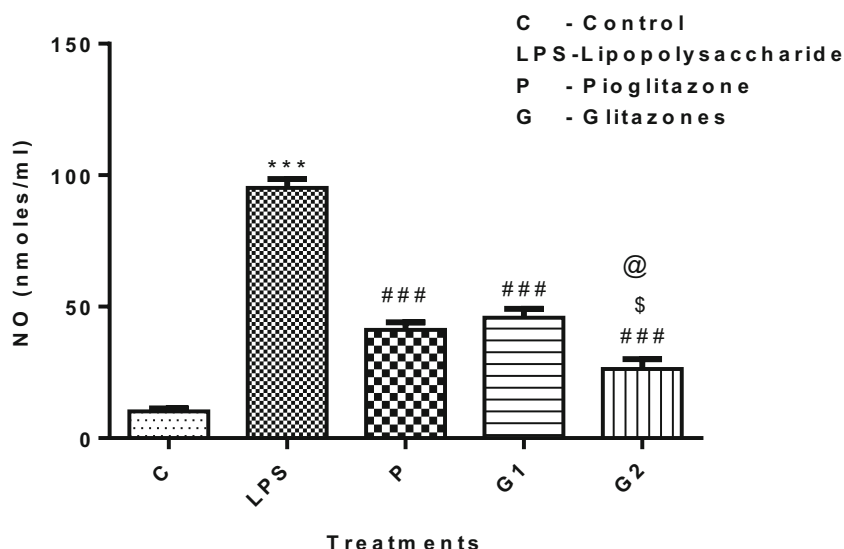


**Fig. 11** Effect of glitazones on NO levels in LPS-intoxicated SH-SY5Y cell lines. Statistical significance was determined by one-way ANOVA followed by Dunnett-t test using Graph pad prism Version 5.0. Values are expressed as mean  $\pm$  SEM, Superscript \*\*\* denotes  $p < 0.001$  vs control, ### denotes  $p < 0.001$  vs LPS, \$ denotes  $p < 0.05$  vs P, @ denotes  $p < 0.05$  vs G1, respectively



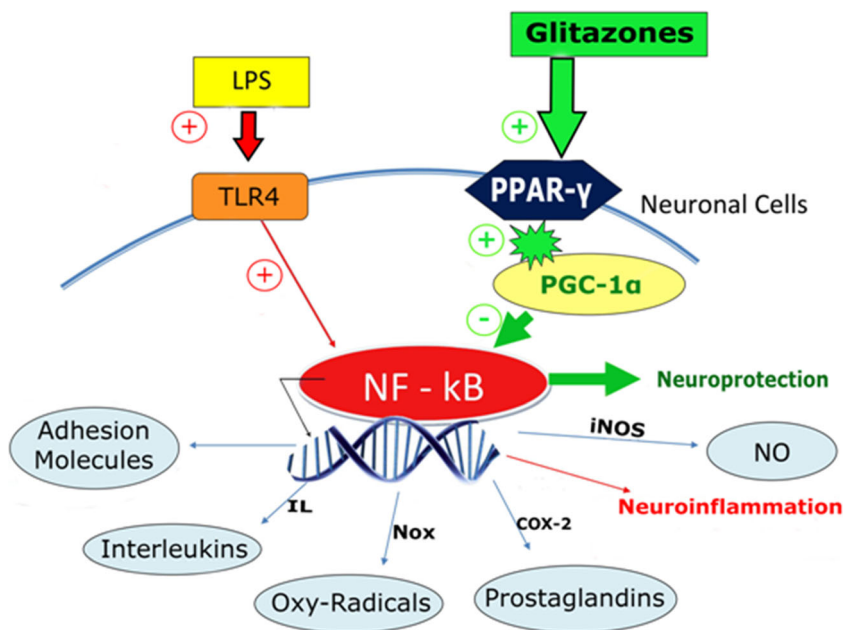
occurring through stimulation of nuclear factor-kappa B (NF- $\kappa$ B) signaling pathway. The activation of NF- $\kappa$ B transcription pathway could increase the transcription of genes associated with cytokine production leads to pro-inflammatory mediator's release [Liu et al. 2017] resulted in neuroinflammation and neuronal death.

LPS also enhances the production of ROS in the neuronal cells (Zhao et al. 2014; Yu et al. 2015). Though several studies are emphasized, the inflammatory mechanism of LPS, the LPS-induced oxidative damage in the brain cells also plays a major role in the several neurodegenerative disorders (Noworyta-Sokolowska et al. 2013). LPS accelerates the ROS formation which causes a significant alteration in NO, malondialdehyde (MDA), reduced glutathione (GSH), superoxide dismutase (SOD), and catalase (CAT) levels in neurons.

Earlier experimental findings have shown that an increased level of pro-inflammatory cytokines (e.g., TNF- $\alpha$ , INF- $\gamma$ , and IL-6) can be the basis of formation of ROS through activating NF- $\kappa$ B transcription (Sharma and Nehru 2015). In our study, we have also observed that treatment with LPS in SH-SY5Y cell lines has increased the LPO and NO level along with pro-inflammatory cytokines. The LPS mainly triggers the ROS through TLR-4 receptor activation followed by stimulation of NF- $\kappa$ B-dependent expression of genes associated with oxidative stress (Leow-Dyke et al. 2012).

The significant increase in the IL-1 $\beta$  and TNF- $\alpha$  level of present experimental findings indicates the LPS accelerated the NF- $\kappa$ B expression in SH-SY5Y cell lines through TLR-4 receptors. It might be caused by the neuroinflammation followed by neurodegeneration which is further evidenced in

**Fig. 12** Proposed mechanism of action of novel glitazones



morphological alterations in LPS-treated cell lines. Interestingly, treatment with novel glitazones (designed as PPAR- $\gamma$  agonist) exhibited significant protective effect in LPS-intoxicated cell lines through attenuation of pro-inflammatory cytokine release and scavenging of oxy-radicals. Research findings are evidenced that agonist activity at PPAR- $\gamma$  receptors elicits anti-neuroinflammatory effect through controlling NF- $\kappa$ B signaling in activated microglia (Choi et al. 2017). A study had shown that deficiency of neuronal PPAR- $\gamma$  receptors increased the intensity of brain damage in response to cerebral ischemia (Zhao et al. 2009). Whereas, agonism of PPAR- $\gamma$  receptors by rosiglitazone exerted neuroprotection through ameliorating the brain cytokine levels in focal ischemic rats (Luo et al. 2006). Activation of PPAR- $\gamma$ -dependent signaling in advanced glycation end toxin-treated human neural stem cells has shown neuroprotection, suggesting that PPAR- $\gamma$  ligands are promising candidates for the therapeutic management of several neurological disorders (Chiang et al. 2017). Interestingly, the neuroprotective mechanism of PPAR- $\gamma$  agonism is mediated through up-regulating the expression of its co-factor, namely PGC-1 $\alpha$ . The activation of PPAR- $\gamma$  results in heterodimerize with RXR and recruits the PGC-1 $\alpha$  to form a regulatory complex (Viswakarma et al. 2010). It could inhibit the mitochondrial and proteasomal dysfunction, oxidative stress, autophagy, neuroinflammation, and apoptosis in neurons through regulating various target genes leading to neuroprotection and neuronal survival.

Therefore, the mechanism of neuroprotective effect of novel glitazones might have attributed through activation of central PPAR- $\gamma$  receptors thereby it would activate the PGC-1 $\alpha$  signaling which was confirmed in the ligand interaction, molecular dynamics, and conformational analysis part of this study. Further, the activation of PGC-1 $\alpha$  signaling would have attenuated the NF- $\kappa$ B expression in neurons resulting in decreased cytokines and free radicals released during neuroinflammatory conditions lead to neuroprotection. The proposed neuroprotective mechanism of synthesized novel glitazones in LPS-induced neuroinflammatory conditions is depicted in Fig. 12.

## Conclusion

Two novel glitazones are rationally designed targeting PGC-1 $\alpha$  via PPAR- $\gamma$  agonism, synthesized, and evaluated for their role in neuroinflammatory conditions. Docking and dynamics study noticeably specified the potential ability of the synthesized compounds to be active towards neuroinflammatory conditions, showing binding interactions at the active site pocket of PPAR- $\gamma$  and in-turn passively changing the conformation of PGC-1 $\alpha$  via PPAR- $\gamma$  activation. The facile synthesis of the compound **G1** and **G2** was accomplished by

sequentially adopting modified Williamson's ether synthesis and Schiff's base formation. The structures of the synthesized compounds were confirmed through the spectral data. The desired neuroprotective activity of the synthesized compounds was assessed in LPS-intoxicated SH-SY5Y cells. The intracellular pro-inflammatory cytokine (TNF- $\alpha$  & IL-1 $\beta$ ) level was measured by ELISA to evaluate the anti-neuroinflammatory ability of synthesized glitazones. The free radical scavenging properties of novel glitazones were assessed by LPO and NO assay. The in vitro results and in silico result cross-correlate for the possibility of PGC-1 $\alpha$  activation thereby possibly enhancing mitochondrial biogenesis. Cognizance study indicates that compounds **G1** and **G2** satisfactorily fulfills the hypothesis, besides compound **G2** showed better results in both in silico and in vitro studies. Altogether, we have identified one candidate compound to investigate further using animal models for its potency and efficacy in neurodegenerative disorders.

**Funding Information** The authors sincerely thank the Department of Science and Technology—Science and Engineering Research Board (DST-SERB), New Delhi for extended financial support to carry out this project (Grant Sanction order No. CRG/2018/002084).

## Compliance with Ethical Standards

**Conflict of Interest** The authors declare that there is no conflict of interest.

## References

- Arai H, Furuya T, Yasuda T, Miura M, Mizuno Y, Mochizuki H (2004) Neurotoxic effects of lipopolysaccharide on nigral dopaminergic neurons are mediated by microglial activation, interleukin-1beta, and expression of caspase-11 in mice. *J Biol Chem* 279(49): 51647–51653
- Bala V, Chhonker YS, Hashim SR (2010) Synthesis and antimicrobial activity of Schiff bases derived from 2-formylphenoxy acetic acid. *Asian J Chem* 22(5):3447–3452
- Cardin S, Guasch E, Luo X, Naud P, Le Quang K, Shi Y, Tardif JC, Comtois P, Nattel S (2012) Role for MicroRNA-21 in atrial profibrillatory fibrotic remodeling associated with experimental postinfarction heart failure. *Circ Arrhythm Electrophysiol* 5(5): 1027–1035
- Chen SD, Yang DI, Lin TK, Shaw FZ, Liou CW, Chuang YC (2011) Roles of oxidative stress, apoptosis, PGC-1 $\alpha$  and mitochondrial biogenesis in cerebral ischemia. *Int J Mol Sci* 12(10):7199–7215
- Chiang MC, Cheng YC, Nicol CJ, Lin CH (2017) The neuroprotective role of rosiglitazone in advanced glycation end product treated human neural stem cells is PPARgamma-dependent. *Int J Biochem Cell Biol* 92:121–133
- Choi MJ, Lee EJ, Park JS, Kim SN, Park EM, Kim HS (2017) Anti-inflammatory mechanism of galangin in lipopolysaccharide-stimulated microglia: Critical role of PPAR- $\gamma$  signaling pathway. *Biochem Pharmacol* 144:120–131
- Clarke SD, Thuillier P, Baillie RA, Sha X (1999) Peroxisome proliferator-activated receptors: a family of lipid-activated transcription factors. *Am J Clin Nutr* 70(4):566–571

- Corona JC, Duchon MR (2015) PPAR $\gamma$  and PGC-1 $\alpha$  as therapeutic targets in Parkinson's. *Neurochem Res* 40(2):308–316
- Delerive P, Fruchart JC, Staels B (2001) Peroxisome proliferator-activated receptors in inflammation control. *J Endocrinol* 169(3):453–459
- DiSabato DJ, Quan N, Godbout JP (2016) Neuroinflammation: the devil is in the details. *J Neurochem* 139(Suppl 2):136–153
- Ewing TJ, Makino S, Skillman AG, Kuntz ID (2001) DOCK 4.0: search strategies for automated molecular docking of flexible molecule databases. *J Comput Aided Mol Des* 15(5):411–428
- Green LC, Wagner DA, Glogowski J, Skipper PL, Wishnok JS, Tannenbaum SR (1982) Analysis of nitrate, nitrite, and [15N]nitrate in biological fluids. *Anal Biochem* 126(1):131–138
- Guasch L, Sala E, Castell-Auví A, Cedó L, Liedl KR, Wolber G, Muehlbacher M, Mulero M, Pinet M, Ardévol A, Valls C, Pujadas G, Garcia-Vallvé S (2012) Identification of PPAR $\gamma$  partial agonists of natural origin (I): development of a virtual screening procedure and in vitro validation. *PLoS One* 7(11):e50816
- Hunter R, Bing G (2007) Agonism of peroxisome proliferator receptor-gamma may have therapeutic potential for neuroinflammation and Parkinson's disease. *Curr Neuropharmacol* 5(1):35–46
- Jin R, Yang G, Li G (2010) Inflammatory mechanisms in ischemic stroke: role of inflammatory cells. *J Leukoc Biol* 87(5):779–789
- Jin J, Albertz J, Guo Z, Peng Q, Rudow G, Troncoso JC, Ross CA, Duan W (2013) Neuroprotective effects of PPAR- $\gamma$  agonist rosiglitazone in N171-82Q mouse model of Huntington's disease. *J Neurochem* 125(3):410–419
- Johri A, Chandra A, Flint Beal M (2013) PGC-1 $\alpha$ , mitochondrial dysfunction, and Huntington's disease. *Free Radic Biol Med* 62:37–46
- Kaja S, Duncan RS, Longoria S, Hilgenberg JD, Payne AJ, Desai NM, Parikh RA, Burroughs SL, Gregg EV, Goad DL, Koulen P (2011) Novel mechanism of increased Ca<sup>2+</sup> release following oxidative stress in neuronal cells involves type 2 inositol-1,4,5-trisphosphate receptors. *Neuroscience* 175:281–291
- Katsouri L, Parr C, Bogdanovic N, Willem M, Sastre M (2011) PPAR $\gamma$  co-activator-1 $\alpha$  (PGC-1 $\alpha$ ) reduces amyloid- $\beta$  generation through a PPAR $\gamma$ -dependent mechanism. *J Alzheimers Dis* 25(1):151–162
- Katsouri L, Lim YM, Blondrath K, Eleftheriadou I, Lombardero L, Birch AM, Mirzaei N, Irvine EE, Mazarakis ND, Sastre M (2016) PPAR $\gamma$ -coactivator-1 $\alpha$  gene transfer reduces neuronal loss and amyloid- $\beta$  generation by reducing  $\beta$ -secretase in an Alzheimer's disease model. *Proc Natl Acad Sci USA* 113(43):12292–12297
- Kulkarni SS, Gediya LK, Kulkarni VM (1999) Three-dimensional quantitative structure activity relationships (3-D-QSAR) of antihyperglycemic agents. *Bioorg Med Chem* 7(7):1475–1485
- Lattke M, Reichel SN, Baumann B (2017) NF- $\kappa$ B-mediated astrocyte dysfunction initiates neurodegeneration. *Oncotarget* 8(31):50329–50330
- Leow-Dyke S, Allen C, Denes A, Nilsson O, Maysami S, Bowie AG, Rothwell NJ, Pinteaux E (2012) Neuronal Toll-like receptor 4 signaling induces brain endothelial activation and neutrophil transmigration in vitro. *J Neuroinflammation* 9:230
- Li Y, Kovach A, Suino-Powell K, Martynowski D, Xu HE (2008) Structural and biochemical basis for the binding selectivity of peroxisome proliferator-activated receptor gamma to PGC-1 $\alpha$ . *J Biol Chem* 283(27):19132–19139
- Li H, Zhang Q, Yang X, Wang L (2017) PPAR- $\gamma$  agonist rosiglitazone reduces autophagy and promotes functional recovery in experimental traumatic spinal cord injury. *Neurosci Lett* 650:89–96
- Liu T, Zhang L, Joo D, Sun SC (2017) NF- $\kappa$ B signaling in inflammation. *Signal Transduct Target Ther* 2. pii: 17023.
- Luo Y, Yin W, Signore AP, Zhang F, Hong Z, Wang S, Graham SH, Chen J (2006) Neuroprotection against focal ischemic brain injury by the peroxisome proliferator-activated receptor-gamma agonist rosiglitazone. *J Neurochem* 97(2):435–448
- Marmolino D, Manto M, Acquaviva F, Vergara P, Ravello A, Monticelli A, Pandolfo M (2010) PGC-1 $\alpha$  down-regulation affects the antioxidant response in Friedreich's ataxia. *PLoS One* 5(4):e10025
- Moreno S, Farioli-Vecchioli S, Cerù MP (2004) Immunolocalization of peroxisome proliferator-activated receptors and retinoid X receptors in the adult rat CNS. *Neuroscience* 123(1):131–145
- Noworyta-Sokołowska K, Górska A, Gołembowska K (2013) LPS-induced oxidative stress and inflammatory reaction in the rat striatum. *Pharmacol Rep* 65(4):863–869
- Ohkawa H, Ohishi N, Yagi K (1979) Assay for lipid peroxides in animal tissues by thiobarbituric acid reaction. *Anal Biochem* 95(2):351–358
- Patel SP, Cox DH, Gollihue JL, Bailey WM, Geldenhuys WJ, Gensel JC, Sullivan PG, Rabchevsky AG (2017) Pioglitazone treatment following spinal cord injury maintains acute mitochondrial integrity and increases chronic tissue sparing and functional recovery. *Exp Neurol* 293:74–82
- Qin W, Haroutunian V, Katsel P, Cardozo CP, Ho L, Buxbaum JD, Pasinetti GM (2009) PGC-1 $\alpha$  expression decreases in the Alzheimer disease brain as a function of dementia. *Arch Neurol* 66(3):352–361
- Qiu D, Li XN (2015) Pioglitazone inhibits the secretion of proinflammatory cytokines and chemokines in astrocytes stimulated with lipopolysaccharide. *Int J Clin Pharmacol Ther* 53(9):746–752
- Rampe D, Wang L, Ringheim GE (2004) P2X7 receptor modulation of beta-amyloid- and LPS-induced cytokine secretion from human macrophages and microglia. *J Neuroimmunol* 147(1-2):56–61
- Randy LH, Guoying B (2007) Agonism of peroxisome proliferator receptor-gamma may have therapeutic potential for neuroinflammation and Parkinson's disease. *Curr Neuropharmacol* 5(1):35–46
- Roeske-Nielsen A, Fredman P, Mansson JE, Bendtzen K, Buschard K (2004) Beta-galactosylceramide increases and sulfatide decreases cytokine and chemokine production in whole blood cells. *Immunol Lett* 91(2-3):205–211
- Róna-Vörös K, Weydt P (2010) The role of PGC-1 $\alpha$  in the pathogenesis of neurodegenerative disorders. *Curr Drug Targets* 11(10):1262–1269
- Rosenberger K, Derkow K, Dembny P, Krüger C, Schott E, Lehnardt S (2014) The impact of single and pairwise Toll-like receptor activation on neuroinflammation and neurodegeneration. *J Neuroinflammation* 11:166
- Shah S, Baseer MAPG (2012) Synthesis and antimicrobial studies of some novel Schiff bases. *Asian J Pharm Clin Res* 5(3):228–232
- Sharma N, Nehru B (2015) Characterization of the lipopolysaccharide induced model of Parkinson's disease: role of oxidative stress and neuroinflammation. *Neurochem Int* 87:92–105
- Skeel RD, Zhang G, Schlick T (1997) A family of symplectic integrators: stability, accuracy, and molecular dynamics applications. *SIAM J Sci Comput* 18(1):203–222
- St-Pierre J, Drori S, Uldry M, Silvaggi JM, Rhee J, Jäger S, Handschin C, Zheng K, Lin J, Yang W, Simon DK, Bachoo R, Spiegelman BM (2006) Suppression of reactive oxygen species and neurodegeneration by the PGC-1 transcriptional coactivators. *Cell* 127(2):397–408
- Swanson CR, Joers V, Bondarenko V, Brunner K, Simmons HA, Ziegler TE, Kennitz JW, Johnson JA, Emborg ME (2011) The PPAR- $\gamma$  agonist pioglitazone modulates inflammation and induces neuroprotection in parkinsonian monkeys. *J Neuroinflammation* 8:91
- Tuckerman M, Beme BJ, Martyna GJ (1992) Reversible multiple time scale molecular dynamics. *J Chem Phys* 97(3):1990–2001
- Tyagi S, Gupta P, Saini AS, Kaushal C, Sharma S (2011) The peroxisome proliferator-activated receptor: a family of nuclear receptors role in various diseases. *J Adv Pharm Technol Res* 2(4):236–240
- Vanommeslaeghe K, Hatcher E, Acharya C, Kundu S, Zhong S, Shim J, Darian E, Guvench O, Lopes P, Vorobyov I, Mackerell AD Jr (2010) CHARMM general force field: a force field for drug-like molecules

- compatible with the CHARMM all-atom additive biological force fields. *J Comput Chem* 31(4):671–690
- Viswakarma N, Jia Y, Bai L, Vluggens A, Borensztajn J, Xu J, Reddy JK (2010) Coactivators in PPAR-regulated gene expression. *PPAR Res* 2010. pii: 250126.
- Wu G, Robertson DH, Brooks CL 3rd, Vieth M (2003a) Detailed analysis of grid-based molecular docking: a case study of CDOCKER-A CHARMM-based MD docking algorithm. *J Comput Chem* 24(13):1549–1562
- Wu X, Milne JL, Borgnia MJ, Rostapshov AV, Subramaniam S, Brooks BR (2003b) A core-weighted fitting method for docking atomic structures into low-resolution maps: application to cryo-electron microscopy. *J Struct Biol* 141(1):63–76
- Yu HY, Cai YB, Liu Z (2015) Activation of AMPK improves lipopolysaccharide-induced dysfunction of the blood-brain barrier in mice. *Brain Inj* 29(6):777–784
- Zhao X, Strong R, Zhang J, Sun G, Tsien JZ, Cui Z, Grotta JC, Aronowski J (2009) Neuronal PPAR $\gamma$  deficiency increases susceptibility to brain damage after cerebral ischemia. *J Neurosci* 29(19):6186–6195
- Zhao Z, Hu J, Gao X, Liang H, Liu Z (2014) Activation of AMPK attenuates lipopolysaccharide-impaired integrity and function of blood-brain barrier in human brain microvascular endothelial cells. *Exp Mol Pathol* 97(3):386–392
- Zhao J, Bi W, Xiao S, Lan X, Cheng X, Zhang J, Lu D, Wei W, Wang Y, Li H, Fu Y, Zhu L (2019) Neuroinflammation induced by lipopolysaccharide causes cognitive impairment in mice. *Sci Rep* 9(1):5790
- Zheng B, Liao Z, Locascio JJ, Lesniak KA, Roderick SS, Watt ML, Eklund AC, Zhang-James Y, Kim PD, Hauser MA, Grünblatt E, Moran LB, Mandel SA, Riederer P, Miller RM, Federoff HJ, Wüllner U, Papapetropoulos S, Youdim MB, Cantuti-Castelvetri I, Young AB, Vance JM, Davis RL, Hedreen JC, Adler CH, Beach TG, Graeber MB, Middleton FA, Rochet JC, Scherzer CR, Global PD Gene Expression (GPEX) Consortium (2010) PGC-1 $\alpha$ , a potential therapeutic target for early intervention in Parkinson's disease. *Sci Transl Med* 2(52):52–73
- Zhu X, Chen C, Ye D, Guan D, Ye L, Jin J, Zhao H, Chen Y, Wang Z, Wang X, Xu Y (2012) Diammonium glycyrrhizinate upregulates PGC-1 $\alpha$  and protects against A $\beta$ 1-42-induced neurotoxicity. *PLoS One* 7(4):e35823
- Zubrys A, Siebenmann CO (1954) Antituberculous isonicotinylhydrazones of low toxicity. *Can J Chem* 33(1):11–14

**Publisher's Note** Springer Nature remains neutral with regard to jurisdictional claims in published maps and institutional affiliations.